Vibrational properties of graphene fluoride and graphane

H. Peelaers,[1,a)] A. D. Hernández-Nieves,[1,2,b)] O. Leenaerts,[1] B. Partoens,[1] and F. M. Peeters[1,c)]
[1]*Departement Fysica, Universiteit Antwerpen, Groenenborgerlaan 171, B-2020 Antwerpen, Belgium*
[2]*Centro Atomico Bariloche, 8400 S. C. de Bariloche, Argentina and CONICET, Centro Atomico Bariloche, 8400 S. C. de Bariloche, Argentina*

(Received 29 October 2010; accepted 14 January 2011; published online 2 February 2011)

The vibrational properties of graphene fluoride and graphane are studied using *ab initio* calculations. We find that both sp^3 bonded derivatives of graphene have different phonon dispersion relations and phonon densities of states as expected from the different masses associated with the attached atoms of fluorine and hydrogen, respectively. These differences manifest themselves in the predicted temperature behavior of the constant-volume specific heat of both compounds. © *2011 American Institute of Physics*. [doi:10.1063/1.3551712]

The chemical modification of graphene[1] is being the focus of increasing interest.[2–8] Radicals such as oxygen, hydrogen, or fluorine atoms can be adsorbed on the surface of graphene. The adsorbed radicals can attach to the graphene layer in a random way, as is the case in graphene oxide,[2] or they can form ordered patterns. The latter is expected to be the case for hydrogen[9,10] and fluorine adsorbates.[11,12] The two-dimensional materials that form in those cases[9] have been named graphane[3,10] and graphene fluoride[4] (or fluorographene[6]), respectively.

Raman spectroscopy provides useful information, and it is being actively used, during the hydrogenation[3] and fluorination[4–7] process of graphene. Both graphane and graphene fluoride are expected to be wide band gap materials.[12] As the energies of the lasers used were lower than the band gap, there was no signature of Raman activity from fully hydrogenated or fully fluorinated regions in those experiments,[3,5–7] and the Raman peaks were associated with graphene.

The main feature in the Raman spectra of pristine graphene is the appearance of the G- and 2D-bands, which appear around 1580 and 2680 cm^{-1}, respectively.[3,13,14] The G-band is associated with the doubly degenerate E_{2g} phonon mode of graphene, while the 2D mode (also called G′) originates from a second-order process, involving two phonons near the K point without the presence of any kind of disorders or defects.[13,14] On the other hand, the presence of defects in the sample (such as adatoms in partially hydrogenated or fluorinated samples) activates additional peaks in the Raman spectra of graphene. This is the case of the D, D′, and D+D′ peaks that appear at 1350, 1620, and 2950 cm^{-1}, respectively.[3,5] These Raman peaks originate from double-resonance processes at the K point in the presence of defects. As the D, D′, and D+D′ peaks involve phonon modes from graphene, they appear at the same frequencies in partially hydrogenated[3] or partially fluorinated samples.[5]

The D and G peaks of graphene provide valuable information on the density of defects. These peaks tend to disappear in the limit of almost fully covered samples as was recently found in graphene fluoride[6,7] but not in previous experiments on graphane[3] or graphite fluorides.[15,16] The first report on Raman signatures of multilayer graphene regions that are fully covered with fluorine atoms was presented in Ref. 8. By using a uv laser with an energy of 5.08 eV, two Raman active modes were detected at 1270 and 1343 cm^{-1}, which are absent for lower laser energies. An infrared active mode was also reported at 1204 cm^{-1}. These modes were correlated with density-functional theory calculations of the phonon frequencies of graphene fluoride at the Γ point.[8]

In this letter, by using first-principles calculations, we investigate the phonon dispersion and the phonon density of states (DOS) of graphene fluoride and graphane. This information can be useful for the interpretation of future experiments on infrared, Raman, and neutron-diffraction spectra of these novel two-dimensional compounds, as well as in the study of a wide variety of other physical properties such as specific heat, thermal expansion, heat conduction, and electron-phonon interaction.

All reported results are obtained with the ABINIT code,[17] using a plane wave basis and Troullier–Martins pseudopotentials.[18] An energy cutoff of 40 hartree was used. A 30 bohr layer of vacuum was used to separate the graphane/fluorographene sheet from its periodical images in order to avoid unphysical interactions. The Brillouin zone was sampled using a $30\times30\times1$ Monkhorst–Pack grid[19] for the electronic structure. Both considered systems are fully relaxed such that all forces are smaller than 5×10^{-5} hartree/bohr and all stresses are smaller than 5×10^{-7} hartree/$bohr^3$. The dynamical properties are calculated within the density-functional perturbation theory,[20] as this allows us to calculate arbitrarily phonon frequencies without requiring the use of a supercell.

Figure 1 shows the calculated phonon dispersion relation for the chair conformation of graphane, as this is the energetically most favorable crystal configuration.[12] The dots indicate the directly calculated frequencies, while the solid line is obtained by using a Fourier based interpolation of the interatomic force constants obtained on a $10\times10\times1$ grid of q-points. As can be seen, the agreement between both calculations is very good. The absence of any imaginary frequency indicates that the chair conformation is stable. It is apparent that the phonons of graphane can be divided into

a)Author to whom correspondence should be addressed. Electronic mail: hartwin.peelaers@ua.ac.be. Present address: Department of Materials, University of California, Santa Barbara, CA 93106-5050, USA.
b)Electronic mail: alexande@cab.cnea.gov.ar.
c)Electronic mail: francois.peeters@ua.ac.be.

 © 2011 American Institute of Physics

Author complimentary copy. Redistribution subject to AIP license or copyright, see http://apl.aip.org/apl/copyright.jsp

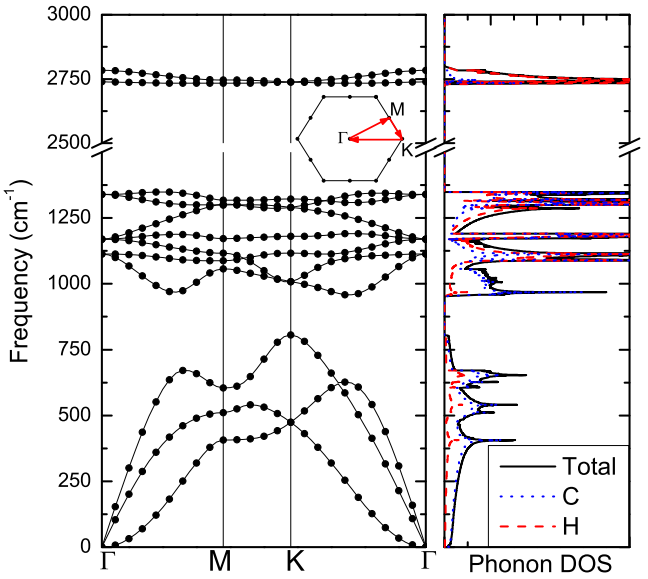

FIG. 1. (Color online) Phonon dispersion of graphane in the chair conformation. The dots are the directly calculated frequencies, and the lines are interpolated values. The inset shows the first Brillouin zone and the wavevector path used. The right-hand side shows the phonon DOS, where the black lines indicate the total DOS, the blue dotted lines the C projected DOS, and the red dashed lines the H projected DOS.

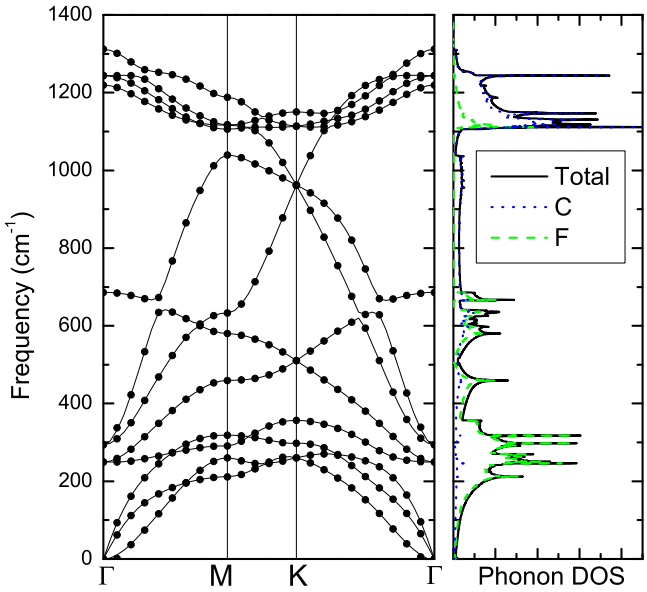

FIG. 2. (Color online) Phonon dispersion of fluorographene in the chair conformation. The dots indicate the directly calculated frequencies and the lines are the interpolated values. The right-hand side shows the phonon DOS, where the black lines indicate the total DOS, the blue dotted lines the C projected DOS, and the green dashed lines the F projected DOS.

low-, intermediate-, and high-frequency groups of phonons. The right-hand side of the figure shows the corresponding DOS, obtained with the interpolated frequency values. The blue dotted line is the DOS projected on the C atoms, and the red dashed line is the projection on the H atoms. From the projected phonon DOS, one can immediately identify the high-frequency modes as dominantly H modes, as can be expected from the C-H stretching modes. The acoustic modes are dominantly C modes, while the intermediate-frequency group of phonons has significant contributions from both types of atoms.

A similar approach can be applied to fluorographene, resulting in the phonon dispersion relation (left) and projected phonon DOS (right) shown in Fig. 2. In the projected DOS, the blue dotted line is the projected DOS on the C atoms, and the green dashed line is the projection on the F atoms. From the dispersion we found that also the chair conformation of fluorographene is stable.

There are substantial differences in the phonon spectra and DOS of graphane and fluorographene. The latter does not show clearly separated groups of phonons. The high-frequency modes are also lower in frequency in comparison with similar modes in graphane because F is heavier than H. In this case, the dominant contribution to the acoustic modes comes from the F atoms, while the high-frequency modes around 1200 cm^{-1} have a clear C character. This behavior is the opposite from the one in graphane because the mass of C atoms is in between the masses of F and H atoms.

The 12 phonon modes of the chair conformation of graphane and graphene fluoride, which has the P-3m1 symmetry (space group 164), belong to four irreducible representations. Frequencies of the different phonon modes at three high-symmetry points of the Brillouin zone (Γ, K, and M) are summarized in Table I. E_g and A_{1g} are Raman active modes, while E_u and A_{2u} are infrared active modes. Our theoretical values of the A_{1g} and the twofold degenerate E_g modes of graphene fluoride at the Γ point, 1244 and 1312 cm^{-1}, are in good agreement with the two Raman active modes found experimentally in Ref. 8 at 1270 and 1345 cm^{-1}, respectively. The same agreement is observed between the infrared active mode A_{2u} at 1219 cm^{-1} and the report of an infrared active mode at 1204 cm^{-1} in Ref. 8.

Using the phonon DOS we can also calculate the constant-volume specific heat of both materials. This is achieved using the expressions described in Ref. 21. One should keep in mind that we work within the harmonic approximation, so the differences with experimental values will become larger for higher temperatures. The hydrogenation of graphene was found to be reversible at 700 K in Ref. 3, while the fluorination of graphene could be reverted at 870 K in Ref. 4. The calculated values of C_v are shown in Fig. 3 where we only report the behavior in the region of stability of each compound. The specific heat of graphane is larger than the one for fluorographene, as can be expected consid-

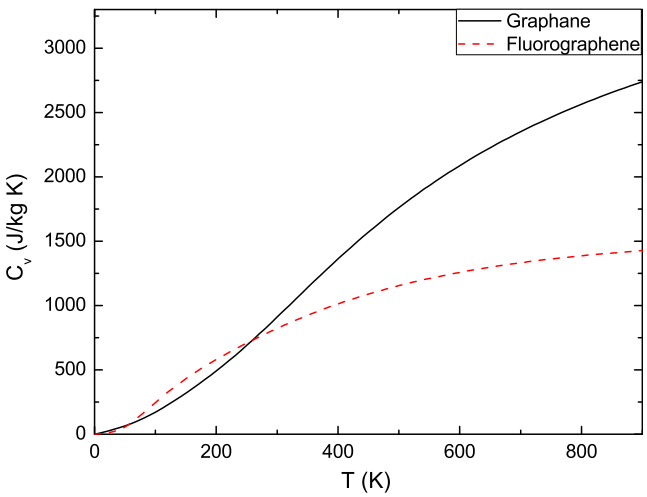

FIG. 3. (Color online) The constant-volume specific heat of graphane (black solid line) and fluorographene (red dashed line). At high temperature, the specific heat of graphane is much larger than the one of fluorographene.

Author complimentary copy. Redistribution subject to AIP license or copyright, see http://apl.aip.org/apl/copyright.jsp

TABLE I. List of symmetries and phonon frequencies at different q-points for graphane and fluorographene. R and I stand for Raman and infrared active modes, respectively.

	Graphane			Fluorographene		
Symmetry (activity)	Γ	M	K	Γ	M	K
A_{2u} (R)	0	407	474	0	211	260
E_u (I)	0	511	474	0	260	260
E_u (I)	0	605	806	0	291	298
E_g (R)	1114	1057	1008	250	318	356
E_g (R)	1114	1088	1008	250	459	510
E_u (I)	1170	1116	1117	294	580	510
E_u (I)	1170	1172	1180	294	633	961
A_{1g} (R)	1170	1299	1290	686	1039	962
E_g (R)	1339	1302	1290	1244	1106	962
E_g (R)	1339	1317	1322	1244	1116	1114
A_{2u} (I)	2739	2733	2739	1219	1117	1114
A_{1g} (R)	2783	2746	2739	1312	1188	1150

ering that the classical limit of the specific heat is given by the Dulong–Petit law and is equal to $3R/M$, where R is the ideal gas constant and M is the molar mass. Because the molar mass of fluorographene is larger than that of graphane, the value of the specific heat will be smaller at high temperatures. To our knowledge there are no experimental measurements yet to compare with. The specific heat of graphene at high temperature (see Fig. 24 of Ref. 22) is in between the specific heats of graphene fluoride and graphane as expected from the Dulong–Petit law.

In summary, the experimental determination of the phonon dispersion relations of graphane and fluorographene can be very useful in the characterization of these materials. It is worth noting that both graphene derivatives are wide band gap materials. This allows us to clearly discriminate, for example, the Raman activity originated from fully fluorinated and fully hydrogenated regions during the synthesis of both compounds by using a laser with appropriate energies.

This work was supported by the Flemish Science Foundation (FWO-Vl), the Belgian Science Policy (IAP), and the collaborative project FWO-MINCyT (Contract No. FW/08/01). A.D.H.-N. is also supported by ANPCyT (under Grant No. PICT2008-2236).

[1]K. S. Novoselov, A. K. Geim, S. V. Morozov, D. Jiang, Y. Zhang, S. V. Dubonos, I. V. Grigorieva, and A. A. Firsov, Science **306**, 666 (2004).
[2]D. A. Dikin, S. Stankovich, E. J. Zimney, R. D. Piner, G. H. B. Dommett, G. Evmenenko, S. T. Nguyen, and R. S. Ruoff, Nature (London) **448**, 457 (2007).
[3]D. C. Elias, R. R. Nair, T. M. G. Mohiuddin, S. V. Morozov, P. Blake, M. P. Halsall, A. C. Ferrari, D. W. Boukhvalov, M. I. Katsnelson, A. K. Geim, and K. S. Novoselov, Science **323**, 610 (2009).
[4]S. H. Cheng, K. Zou, F. Okino, H. R. Gutierrez, A. Gupta, N. Shen, P. C. Eklund, J. O. Sofo, and J. Zhu, Phys. Rev. B **81**, 205435 (2010).
[5]F. Withers, M. Dubois, and A. K. Savchenko, Phys. Rev. B **82**, 073403 (2010).
[6]R. R. Nair, W. C. Ren, R. Jalil, I. Riaz, V. G. Kravets, L. Britnell, P. Blake, F. Schedin, A. S. Mayorov, S. Yuan, M. I. Katsnelson, H. M. Cheng, W. Strupinski, L. G. Bulusheva, A. V. Okotrub, K. S. Novoselov, A. K. Geim, I. V. Grigorieva, and A. N. Grigorenko, Small **6**, 2877 (2010).
[7]J. T. Robinson, J. S. Burgess, C. E. Junkermeier, S. C. Badescu, T. L. Reinecke, F. K. Perkins, M. K. Zalalutdniov, J. W. Baldwin, J. C. Culbertson, P. E. Sheehan, and E. S. Snow, Nano Lett. **10**, 3001 (2010).
[8]B. Wang, J. R. Sparks, H. R. Gutierrez, F. Okino, Q. Hao, Y. Tang, V. H. Crespi, J. O. Sofo, and J. Zhu, Appl. Phys. Lett. **97**, 141915 (2010).
[9]M. H. F. Sluiter and Y. Kawazoe, Phys. Rev. B **68**, 085410 (2003).
[10]J. O. Sofo, A. S. Chaudhari, and G. D. Barber, Phys. Rev. B **75**, 153401 (2007).
[11]J.-C. Charlier, X. Gonze, and J.-P. Michenaud, Phys. Rev. B **47**, 16162 (1993).
[12]O. Leenaerts, H. Peelaers, A. D. Hernandez-Nieves, B. Partoens, and F. M. Peeters, Phys. Rev. B **82**, 195436 (2010).
[13]L. M. Malard, M. A. Pimenta, G. Dresselhaus, and M. S. Dresselhaus, Phys. Rep. **473**, 51 (2009).
[14]A. C. Ferrari, J. C. Meyer, V. Scardaci, C. Casiraghi, M. Lazzeri, F. Mauri, S. Piscanec, D. Jiang, K. S. Novoselov, S. Roth, and A. K. Geim, Phys. Rev. Lett. **97**, 187401 (2006).
[15]V. Gupta, T. Nakajima, Y. Ohzawa, and B. Žemva, J. Fluorine Chem. **120**, 143 (2003).
[16]Graphite fluorides were first synthesized in 1934 [O. Ruff and O. Bretschneider, Z. Anorg. Allg. Chem. **217**, 1 (1934)]. However, only recently in Refs. 6 and 7 it was possible to isolate monolayers of this material.
[17]X. Gonze, B. Amadon, P.-M. Anglade, J.-M. Beuken, F. Bottin, P. Boulanger, F. Bruneval, D. Caliste, R. Caracas, and M. Côté, Comput. Phys. Commun. **180**, 2582 (2009).
[18]N. Troullier and J. L. Martins, Phys. Rev. B **43**, 1993 (1991).
[19]H. J. Monkhorst and J. D. Pack, Phys. Rev. B **13**, 5188 (1976).
[20]S. Baroni, S. de Gironcoli, A. Dal Corso, and P. Giannozzi, Rev. Mod. Phys. **73**, 515 (2001).
[21]C. Lee and X. Gonze, Phys. Rev. B **51**, 8610 (1995).
[22]N. Mounet and N. Marzari, Phys. Rev. B **71**, 205214 (2005).

Author complimentary copy. Redistribution subject to AIP license or copyright, see http://apl.aip.org/apl/copyright.jsp